ICES Journal of
Marine Science

ICES Journal of Marine Science (2012), 69(5), 852–863. doi:10.1093/icesjms/fss056

# Variability in Atlantic water temperature and transport at the entrance to the Arctic Ocean, 1997–2010

Agnieszka Beszczynska-Möller[1]*, Eberhard Fahrbach[1], Ursula Schauer[1], and Edmond Hansen[2]

[1]*Alfred Wegener Institute for Polar and Marine Research, Am Handelshafen 12, 27570 Bremerhaven, Germany*
[2]*Norwegian Polar Institute, Fram Centre, Hjalmar Johansens gt. 14, NO-9296 Tromsø, Norway*

**Corresponding author: tel: +49 4714 8311807; fax: +49 4714 8311797; e-mail: agnieszka.beszczynska-moeller@awi.de*

Beszczynska-Möller, A., Fahrbach, E., Schauer, U., and Hansen, E. 2012. Variability in Atlantic water temperature and transport at the entrance to the Arctic Ocean, 1997–2010. – ICES Journal of Marine Science, 69: 852–863.

Received 14 June 2011; accepted 19 February 2012; advance access publication 18 April 2012.

The variability in Atlantic water temperature and volume transport in the West Spitsbergen Current (WSC), based on measurements by an array of moorings in Fram Strait (78°50′N) over the period 1997–2010, is addressed. The long-term mean net volume transport in the current of 6.6 ± 0.4 Sv (directed northwards) delivered 3.0 ± 0.2 Sv of Atlantic water (AW) warmer than 2°C. The mean temperature of the AW inflow was 3.1 ± 0.1°C. On interannual time-scales, a nearly constant volume flux in the WSC core (long-term mean 1.8 ± 0.1 Sv northwards, including 1.3 ± 0.1 Sv of AW warmer than 2°C, and showing no seasonal variability) was accompanied by a highly variable transport of 2–6 Sv in the offshore branch (long-term mean of 5 ± 0.4 Sv, strong seasonal variability, and 1–2 Sv of warm AW). Two warm anomalies were found in the AW passing through Fram Strait in 1999–2000 and 2005–2007. For the period 1997–2010, there was a positive linear trend in the AW mean temperature of 0.06°C year$^{-1}$, but no statistically significant trend was observed in the AW volume transport. A possible impact of warming on AW propagation in the Arctic Ocean and properties of the outflow to the North Atlantic are also discussed.

**Keywords:** Fram Strait, Atlantic water, West Spitsbergen Current, Oceanic transports, moorings, Arctic Ocean.

## Introduction

Exchanges between the North Atlantic and the Arctic Ocean result in the most dramatic water mass conversions in the world's oceans. On the way through the Nordic Seas into the Arctic Ocean, warm and saline Atlantic waters undergo processes of cooling, freezing, and melting, where shallow fresher waters, ice, and saline deep waters are produced. The outflow from the Nordic Seas to the south provides the initial driver of the global thermohaline circulation cell. Knowledge of these fluxes and understanding of the modification processes are major prerequisites for the quantification of the rate of overturning within the large circulation cells of the Arctic and Atlantic Oceans. It is also a basic requirement for understanding the role of these ocean areas in climate variability on interannual to decadal time-scales.

During the past decade, extraordinarily warm Atlantic water has been reported progressing from the eastern North Atlantic into the Nordic Seas and farther towards the Arctic Ocean (Holliday *et al.*, 2008, 2009). Preceded by the warming in early 1990s, this constitutes a prolonged period of increased heat input to the Arctic Ocean. The earlier warm anomaly was mostly generated inside the Nordic Seas as a response to higher air temperatures and reduced heat loss (Furevik, 2001), and to a lesser extent enhanced by the stronger Atlantic water (AW) inflow (Karcher *et al.*, 2003). In contrast, the warming of the past decade had its origins in the increased northward advection of subtropical waters related to a westward shift of the Subarctic Front and a contraction of the Subpolar Gyre (Hátún *et al.*, 2005; Bersch *et al.*, 2007). As a consequence, since 1995, the anomalously warm and saline waters have been transported by the intensified North Atlantic Current into the Nordic Seas (Holliday *et al.*, 2008).

After passing over the Greenland–Scotland Ridge, most AW continues as the Norwegian Atlantic Current (NwAC). Orvik and Niiler (2002) showed that NwAC maintains the two-branch structure throughout the Nordic Seas towards Fram Strait, with a wide wedge of AW between the main cores. Both branches follow topography, the eastern NwAC branch (also referred to as the Norwegian Atlantic Slope Current, NwASC) constituting a coherent barotropic current along the continental slope west of Norway. The western branch of NwAC (known also as the Norwegian Atlantic Front Current) flows as a baroclinic, topographically steered jet along the underwater ridges (Mork and Skagseth, 2010). Taking topography into account, Nøst and

Isachsen (2003) reproduced a two-core structure in a flowfield based on hydrography. North of Norway, the eastern NwAC branch bifurcates into the stream of AW entering the Barents Sea and the West Spitsbergen Current (WSC) carrying the warm, saline AW farther north above the shelf slope west of Svalbard. Hydrographic observations by Walczowski *et al.* (2005) suggest that because of the bottom topography, the northern extension of the western NwAC branch flowing along the Knipovich Ridge converges with the WSC (the northward extension of the eastern NwAC branch) in Fram Strait between 77° and 77°30′N. However, only a part of this joint AW flow continues into the Arctic Ocean, and a significant amount recirculates directly in Fram Strait and returns south to the Nordic Seas (Schauer *et al.*, 2004).

Fram Strait is the sole conduit conveying warm anomalies from the northern Atlantic to the Arctic Ocean. A recent study by Mauritzen *et al.* (2011) quantifies the water mass transformation within the northernmost limb of the Meridional Overturning Circulation, going from the North Atlantic through the Nordic Seas and Arctic Ocean. The median temperature of the AW flow changes from 7–10°C at the entrance in the Nordic Seas to 6–6.5°C at the Barents Sea opening, to 3–3.5°C as the AW enters the Arctic Ocean in Fram Strait. The same study estimates the volume transport through the Barents Sea opening as 1.6 Sv for waters warmer than 4°C. However, the AW passing through the shallow Barents Sea completely loses its signature as a result of atmospheric cooling and enters the Arctic Ocean with temperature close to 0°C (Schauer *et al.*, 2002). Smedsrud *et al.* (2010) showed, using the updated volume and heat budgets, that most of the heat carried by the AW flow is already lost to the atmosphere in the southern Barents Sea, so does not reach the Arctic Ocean.

In contrast, in the deep Fram Strait, the upper part of the AW becomes transformed into a less saline surface layer by melting sea ice and mixing with fresher surface water of Arctic origin, so the AW preserves its warm core, losing less heat to the atmosphere. Several authors (e.g. Polyakov *et al.*, 2005; Dmitrenko *et al.*, 2008) showed that warm anomalies passing through Fram Strait can be traced further in the Arctic Ocean Boundary Current in the Eurasian Basin. According to the recent estimate by Schauer *et al.* (2008), from 1997 to 2006, the AW inflow through Fram Strait on an interannual time-scale carried between 26 and 50 TW of heat into the Arctic Ocean. To gain more detailed knowledge of spatial and temporal changes of this inflow, the present study addresses the variability of the AW temperature and volume transport on different time-scales from seasonal to interannual.

## Data and methods

Since 1997, year-round velocity, temperature, and salinity measurements have been carried out in Fram Strait with moored instruments. Hydrographic sections exist since 1980. The estimates of mass and heat fluxes through the strait are obtained using a combination of both datasets. From 1997 to 2000, there was intensive fieldwork under the project VEINS (Variability of Exchanges in Northern Seas), which was continued under national programmes. From 2003 to 2005, the work was carried out as part of ASOF–N (Arctic–Subarctic Ocean Fluxes North) project, and from 2006 to 2009, measurements in Fram Strait were performed under the DAMOCLES (Developing Arctic Modelling and Observing Capabilities for Long-term Environment Studies) integrated project. From 2009 on, the observational programme was continued within the EU ACOBAR project. The mooring line is a joint effort between the Alfred Wegener Institute (AWI) and the Norwegian Polar Institute (NPI).

The array of deep oceanographic moorings (14 moorings before 2002, 16 thereafter) at 78°50′N has been maintained for 13 years (Schauer *et al.*, 2008), covering the whole strait from the shelf west of Svalbard through the deep part to the eastern Greenland shelf (Figure 1). The eastern and central set of moorings is operated by AWI (10 before and 12 after 2002), the western four moorings are maintained by NPI, and all are exchanged yearly within a similar period. The moored array covers the section 300 km wide with a spatial resolution from ~10 km at the upper shelf slope to ~30 km in the deep area. The array of classical moorings has evolved since the beginning of observations on an optimized set-up with an enhanced number of moorings and standard depths of instruments. In 2002, the array was redesigned and augmented with two additional moorings in the deepest part of Fram Strait and instrumentation at the lower boundary of the AW layer. Currently, all moorings are instrumented at standard levels: subsurface (~50 m); the level of the AW layer (~250 m); the level of the AW lower boundary (~750 m); the level of the deep water (~1500 m where available); and the near-bottom level (~10 m above the bottom). Through all deployments, each subsurface mooring carried three to seven instruments including rotor and acoustic current meters from Aanderaa Instruments (RCM7, RCM8, and RCM11), acoustic current profilers from RD Instruments (WH and QM ADCP), temperature and salinity sensors from Sea-Bird Electronics Inc. (SBE37 and SBE16), and bottom pressure recorders from Sea-Bird (SBE26). Current meters are equipped with temperature sensors, and most also with pressure sensors. In 2010, point current meters in the Atlantic layer at the eastern eight moorings were replaced with ADCPs to measure the vertical structure of the flow in the upper 250 m with high resolution, but these data are not available yet.

Detailed description of data accuracy and treatment can be found in Fahrbach *et al.* (2001) and Schauer *et al.* (2004). To summarize, the current and temperature data were collected at 1- or 2-h intervals, despiked, low-pass filtered with a cut-off period of 40 h to remove a tidal signal, and averaged at 6-h intervals. In the present study, the monthly averages of temperature and meridional current time-series from all instrumented points were first calculated then interpolated onto a regular grid with a horizontal step of 1 km and a vertical step of 5 m, using kriging (a method equivalent to optimal interpolation). The volume transport was obtained by integrating monthly gridded fields of the meridional current component in different temperature classes.

Atlantic water was defined as warmer than 2°C, using the range coinciding with the warm AW in a water mass classification given by Schlichtholz and Houssais (2002). As the quality of salinity data is not sufficient to analyse the transport in temperature–salinity classes or to allow more sophisticated classification of water masses based on density classes, all water warmer than 2°C will be referred to as AW. However, high-resolution conductivity, temperature, depth (CDT) summer sections suggest that the depth of the 2°C isotherm in the eastern and central Fram Strait mostly coincides with the depth of isopycnal $\sigma_\Theta = 27.97$, which defines the AW boundary in temperature–

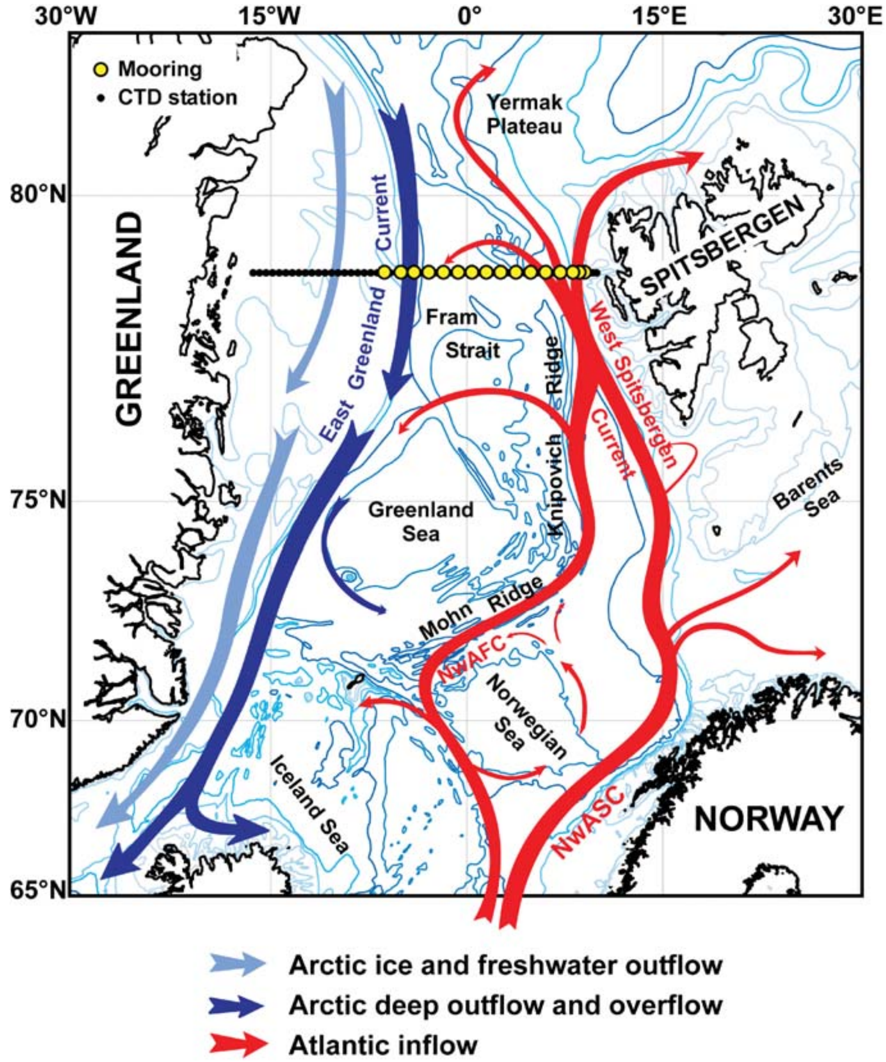


**Figure 1.** A circulation scheme for the Nordic Seas and Fram Strait, showing the locations of the moored array and the annually repeated hydrographic section.

density space in the water mass classification proposed by Rudels *et al.* (2005). This supports our choice of the AW temperature criterion to define the lower boundary of the AW layer. The AW upper boundary defined by isopycnal $\sigma_\Theta = 27.7$ cannot be resolved by observations at the moored array, so the AW layer was assumed to extend to the surface (when warmer than 2°C). To study interannual variability, the winter-centred annual averages of temperature and volume transport (each annual mean is an average of July to June data) were applied to reflect the deployment periods and to take the seasonal cycle better into account. All long-term means are given with the standard error for the 95% confidence interval.

To generate information on salinity variations associated with the observed variability of the AW temperature, though on coarser time-scales, summer hydrographic sections were used. CTD ship-borne measurements are repeated annually along the mooring line in the northern Fram Strait between the shelf west of Svalbard and the East Greenland shelf, usually between July and September. The hydrographic surveys and instrumentation are described in Fahrbach *et al.* (2007).

## Results

### Long-term means of temperature and volume transport in the WSC

The long-term averages of current vectors measured at different depths, overlaid on bottom topography in Fram Strait, are presented in Figure 2a. The three easternmost moorings between 8° and 8°40′E are located above the upper shelf slope, and they represent the steady flow in the core of the WSC. Being the continuation of the strongly barotropic, topographically steered NwASC, which flows above the Norwegian shelf slope and continues along the western Barents Sea slope (Orvik and Niiler, 2002; Skagseth *et al.*, 2004), the WSC core reveals similar dynamic properties, very weak vertical current shear, and steady flow direction along the isobaths. In Figure 2c, the core of the flow is indicated by the mean current velocity exceeding 15 cm s$^{-1}$, with a maximum of >20 cm s$^{-1}$ above the 700 m isobath. The highest mean temperature (~4.4°C) along the whole section is at the same location (Figure 2b). Temperature decreases from this maximum in both onshore and offshore directions. The eastward decrease in the mean temperature is related to the heat exchange

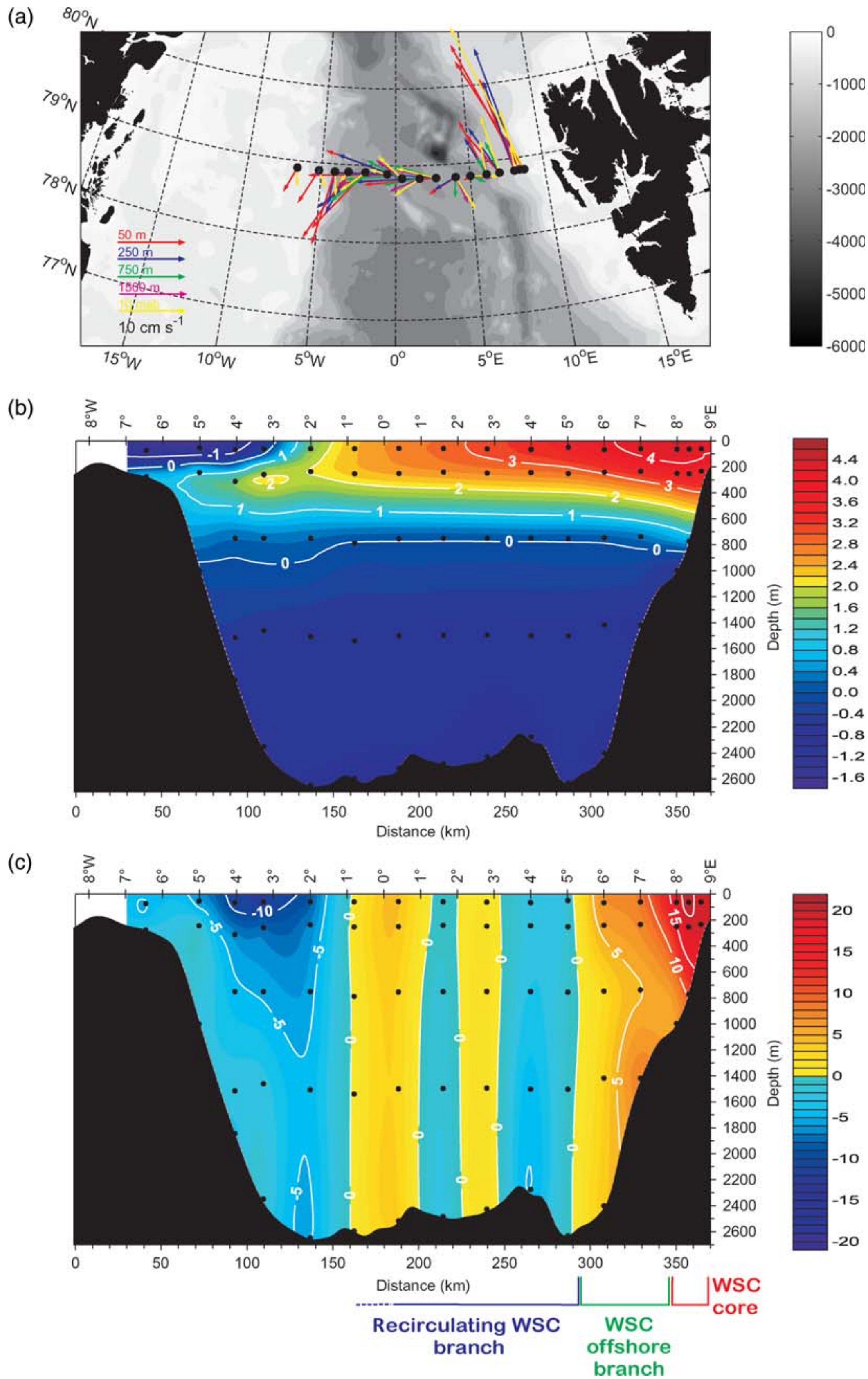


**Figure 2.** (a) Long-term mean (2002–2008) current vectors measured at the moored array at different depths, overlaid on the bottom topography, (b) long-term mean temperature (°C) measured by moored instruments, and (c) mean velocity (cm $s^{-1}$) of the cross section (meridional) current component in Fram Strait.

through the Arctic Front, separating the WSC from the cold waters on the West Spisbergen Shelf (Saloranta and Haugan, 2004; Tverberg and Nøst, 2009).

The offshore WSC branch, characterized by a meridional current of between 0 and 15 cm $s^{-1}$ and a stronger vertical shear (Figure 2b), evolves from the northward extension of the western branch of the NwAC. The AW carried in the western NwAC by the baroclinic jet follows the Mohn and Knipovich Ridges towards Fram Strait, then converges with the WSC upstream of the moored section (Orvik and Niiler, 2002; Walczowski *et al.*, 2005). Although a separation between the WSC core and its offshore branch is clearly visible in the mean current vectors (Figure 2a) and through the strong horizontal gradient of the meridional current component (Figure 2c), its signature in the temperature field is less obvious (Figure 2b). A strong vertical temperature gradient marks the lower boundary of the AW layer, located between 400 and 500 m for the warm AW (temperature higher than 2°C), and aligned along 800 m when the cold AW fraction (with temperatures of 0–2°C, after Schlichtholz and Houssais, 2002) is included. Water warmer than 2°C spreads also in the central, deepest part of the strait (east of 2°W), occupying the upper 300–400 m layer. The mean current vectors (Figure 2a) and variable bands of northward and southward meridional current component in this region (Figure 2c) reveal meanders of the westward recirculation of the AW (also called Return Atlantic Water, RAW), which originates from the WSC. Farther west, the relatively warm RAW is flooded by the cold and less saline Arctic Ocean surface water carried south by the East Greenland Current.

Older papers refer to the WSC core as the Svalbard branch, and the offshore branch was defined as a flow following the westward rim of the Yermak Plateau, and hence called the Yermak Branch (Manley, 1995; Schauer *et al.*, 2004). However, in the Yermak Branch, the signature of the warm AW is strongly weakened by the enhanced tidal mixing (Padman *et al.*, 1992). Moreover, a part of the AW from the offshore branch joins the local circulation loop around the Molloy Deep and/or recirculates westwards as baroclinic eddies, so as a consequence never reaches the Yermak Plateau north of Fram Strait. The partitioning of the AW derived from the WSC offshore branch between the flow towards the Yermak Plateau and a direct recirculation in Fram Strait is still an open question.

The long-term mean net volume transport in the WSC for the period 1997–2010 was estimated as $6.6 \pm 0.4$ Sv (in the whole water column), and the net flux of the AW warmer than 2°C was estimated as $3.0 \pm 0.2$ Sv. Quantification of the volume transport in the WSC in thermal space (Figure 3) reveals a dominant temperature mode of 2.5–4°C with transport of ~2 Sv (slightly <1/3 of the total transport and ~2/3 of the AW inflow). The volume transport decreased quickly towards higher temperature classes. The mean temperature of the AW inflow in the WSC was $3.1 \pm 0.1$°C, with a slight difference between the WSC core and offshore branches, where it was estimated as $3.3 \pm 0.1$ and $3.0 \pm 0.1$°C, respectively. The mean volume transport confined to the WSC core was $1.8 \pm 0.1$ Sv (total net transport), and it included $1.3 \pm 0.1$ Sv of AW warmer than 2°C. The offshore WSC branch carried on average $4.9 \pm 0.4$ Sv (total net transport), to which the AW flux contributed $1.7 \pm 0.1$ Sv, some 35%. All net volume transports were directed to the north.

## Seasonal variability in AW temperature and volume transport

The upper layer temperature in Fram Strait is characterized by a strong seasonal signal. Figure 4a is a spatial distribution of the peak amplitude of the temperature seasonal signal composed of annual and semiannual harmonics (note that the fraction of variance explained by the semiannual component is negligible). White numbers overlaid on a temperature map indicate a percentage of variance explained by the seasonal signal at each measurement point. In the uppermost layer, at a depth of ~50 m, >50% of the temperature variability in both branches is explained by seasonal variations. In deeper layers, a prominent difference can be seen between the WSC core, where the seasonal signal reaches the bottom (and at a depth of ~250 m still stands for 20–30% of variance), and the offshore branch, where it is confined to the upper few hundred metres. Despite these differences, the strong seasonal modulation of temperature can be recognized across the Fram Strait as far as AW is present at a depth of 250 m

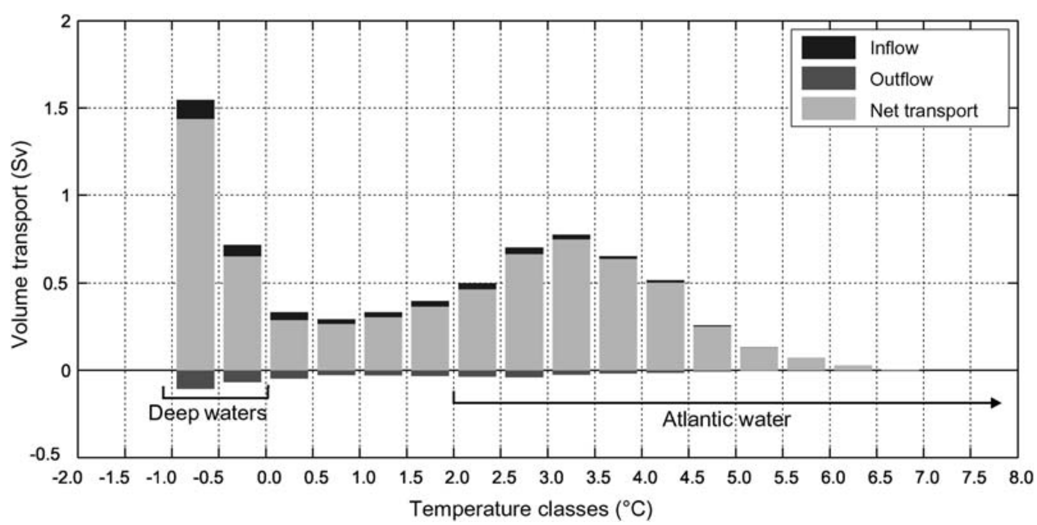


**Figure 3.** Long-term average total volume transport (Sv) in the WSC binned in temperature classes.

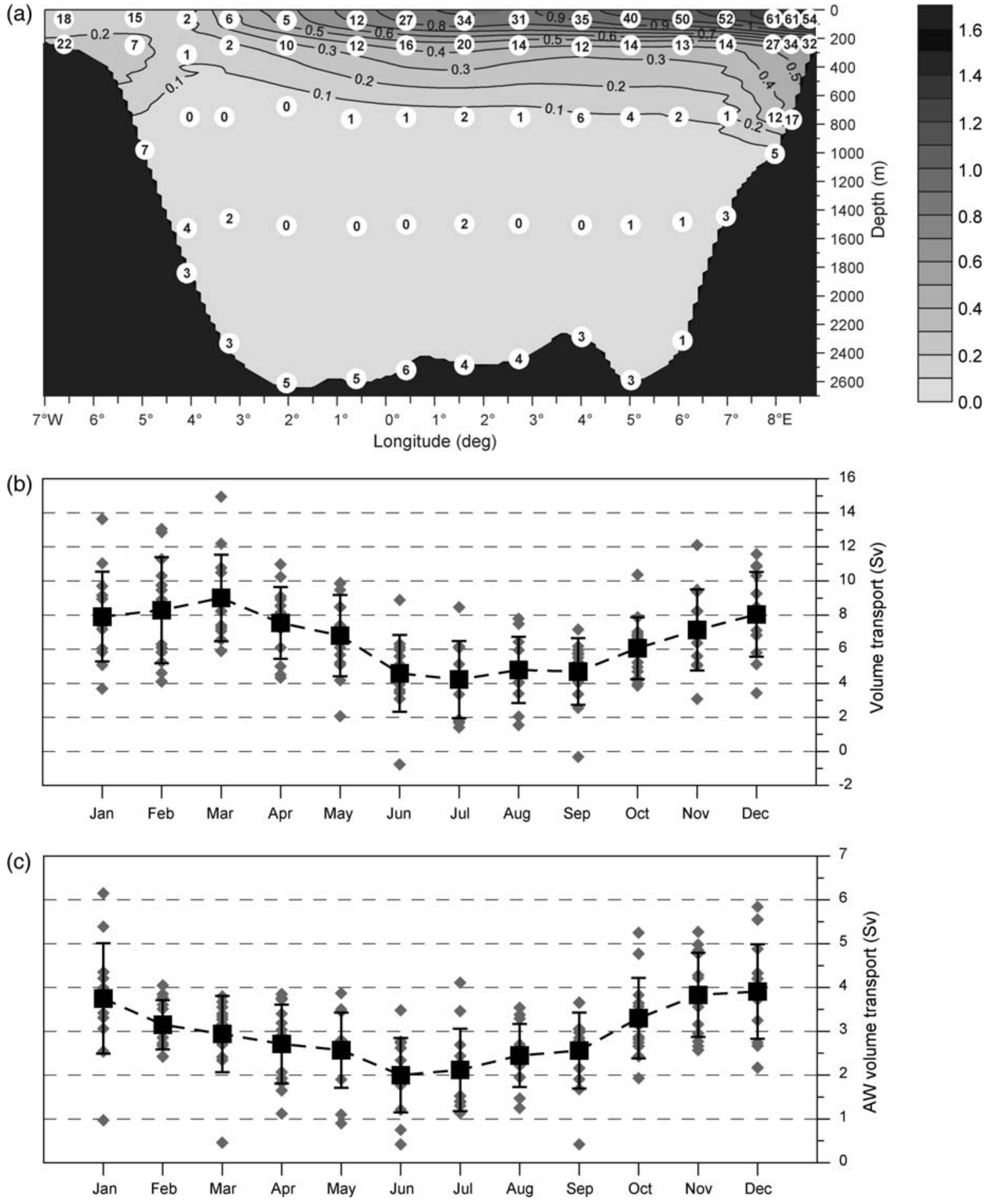


**Figure 4.** (a) Spatial distribution of the peak amplitude of seasonal temperature signal composed of annual and semiannual harmonics. Numbers in white circles represent the amount of variance explained by the seasonal signal at each measurement point. (b) Annual cycle of the monthly averaged total net volume transport, and (c) AW net volume transport in the WSC. Diamonds represent individual monthly means, and large black squares show the long-term mean annual cycle and its standard deviation.

(Figure 5a). The mean seasonal cycle can be subject to interannual variation (von Schuckmann *et al.*, 2009). Long time-series of the mean AW temperature in the WSC (Figure 6a) reveal changes in temperature maxima in early autumn (September–October) overlying the overall positive trend and may indicate year-to-year shifts in the seasonal cycle of temperature.

A significant seasonality is also observed in the volume transport of the WSC. The total volume transport (Figure 4b) is

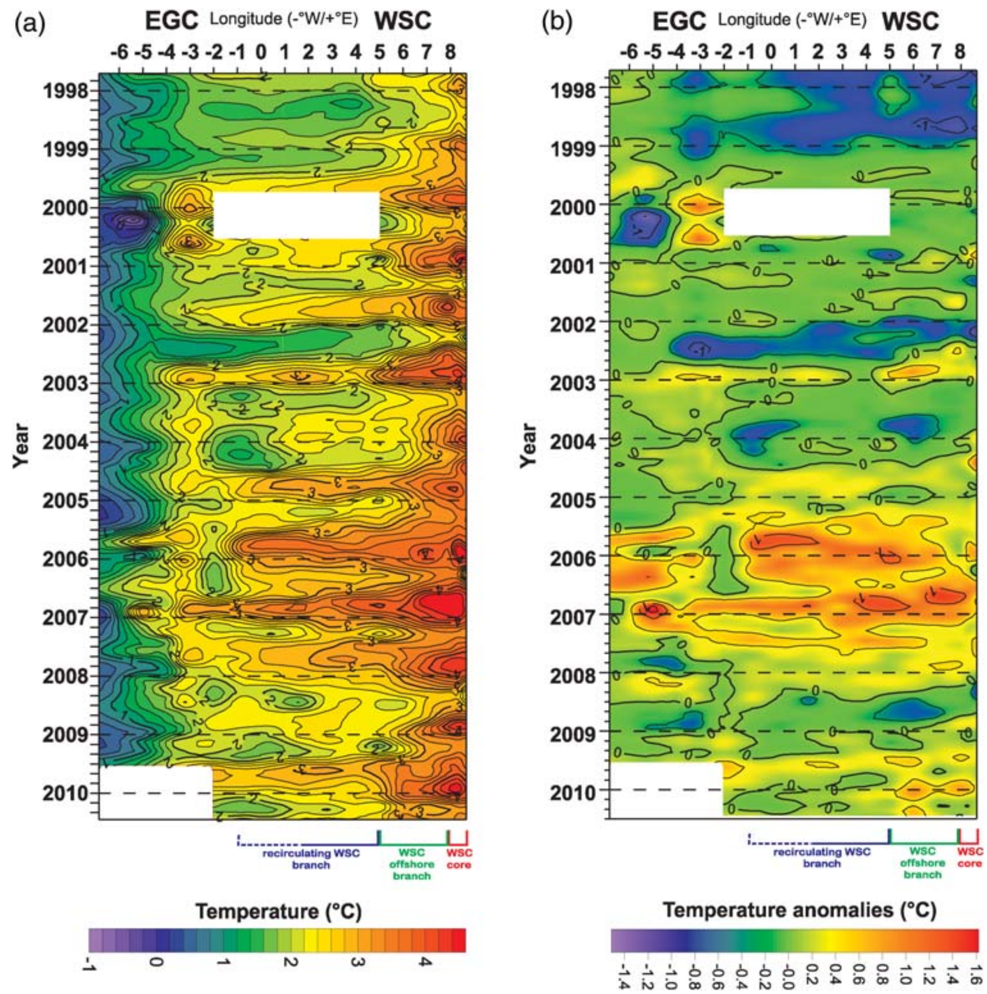


**Figure 5.** Spatio-temporal diagram of monthly means of (a) temperature at 250 m, and (b) temperature anomalies from a mean seasonal cycle measured at the moored array in Fram Strait.

maximum in March (8 Sv) and minimum in July (4.2 Sv) with distinctly low transport in summer (June–September). The peak-to-peak amplitude of the seasonal variations amounts to ~60% of the mean volume transport. The AW inflow of water warmer than 2°C has a slightly different seasonal cycle (Figure 4c). The lowest AW inflow is observed in June (2 Sv), and the strong AW transport dominates through late autumn/winter (3.8–3.9 Sv). The peak amplitude of the seasonal cycle is thus ±1 Sv for the mean AW transport. A shift in the maximum of the AW volume transport towards earlier months (when compared with the total volume transport in the WSC) results from spatial variability and seasonal cycles of the AW temperature. The thickness of the AW layer warmer than 2°C decreases in winter, and in terms of the AW volume transport, a smaller cross-sectional area covered by the AW is not compensated for by a stronger northward current in late winter.

## Variations in AW temperature and transport on monthly to interannual scales

The spatio-temporal variability in the AW temperature in Fram Strait at a depth of 250 m, based on monthly averaged data, is presented in Figure 5a. The most prominent feature is the seasonal cycle, clearly visible across the whole width of the strait occupied by the AW. A spreading of the warm AW westwards is apparent in the second half of the year, between late summer and early winter. Two distinctive warming periods are evident in the spatial distribution of the AW through the strait. The first was in late 1999–2000, unfortunately during a period with no mooring coverage in the deepest part of the strait. However, a signature of these warm waters was clearly visible in the EGC in the western Fram Strait (as far as 4°W), as well as in the central part of the strait during the months before and after the gap in the data. The second warming period started in late 2004 and continued until 2008, when there was a significant temperature decrease in the entire AW layer in the strait. During the peak of the second warming (in September 2006), the anomalously warm AW, with temperatures >3°C, reached the East Greenland Current and the upper slope east of Greenland. On the eastern side of the WSC, the AW warmer than 3°C was present at a depth of 250 m all through the year, in contrast to earlier years when its occurrence was seasonal. As the seasonal signal strongly masks interannual variations, it is useful to separate the temperature anomalies from the long-term averaged seasonal cycle.

In Figure 5b, the spatio-temporal diagram of temperature anomalies, calculated about the mean seasonal cycle during the years 1997–2010, clearly reveals subsequent cold and

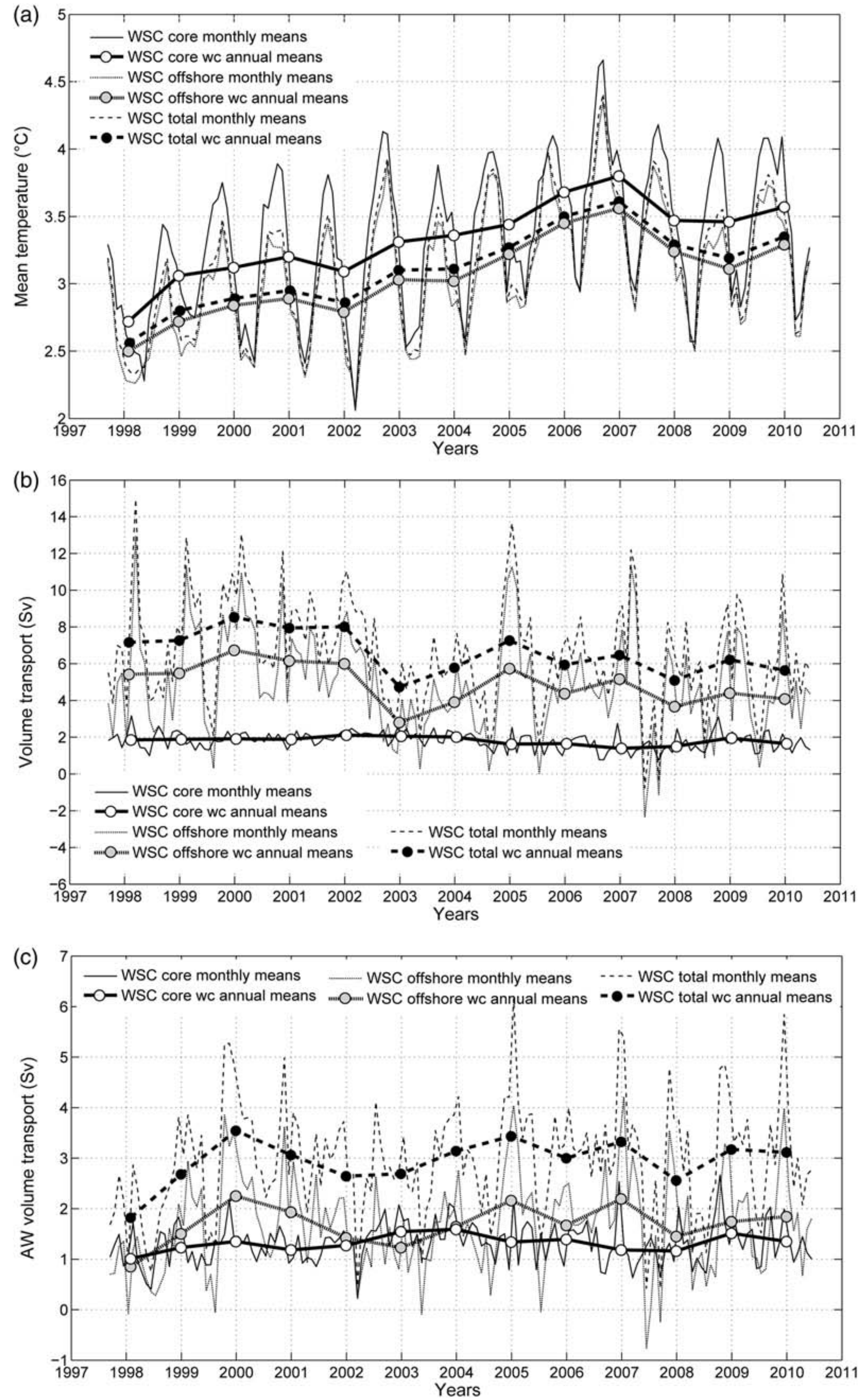


**Figure 6.** Monthly and winter-centred annual means of (a) AW temperature, (b) volume transport, and (c) AW volume transport. Separate lines represent data for the WSC (dashed line, black circles), the WSC core (solid line, white circles), and the offshore branch (dot line, grey circles).

warm periods in the northern Fram Strait. The amplitude of the first warming was smaller than that of the second warming, when temperature anomalies >1°C were observed in the eastern and central part of Fram Strait. An intermittent pattern of warm anomaly in winter 2005/2006 suggests that the warmer water present above the East Greenland Shelf originated from the AW recirculation north of Fram Strait, whereas the continuous spreading of the warm anomaly in winter 2006/2007 across the whole section suggests stronger recirculation directly in Fram Strait. Although the last warming was succeeded by the slightly negative temperature anomaly in 2008, the AW temperature has been rising anew since summer 2009, resulting in a weakly positive anomaly.

Monthly and winter-centred annual means of the AW temperature shown in Figure 6a illustrate a continuous increase between 1997 and 2006, with similar variability in both WSC branches. The lowest annual mean AW temperature of 2.5°C was in 1997, whereas in 2006, the peak of 3.6°C was reached. During the recent cold period in 2008–2009, the differences between the mean temperature of the AW in the WSC core and in the offshore branch were largest (up to 0.8–0.9°C). Month-to-month variations of the AW mean temperature were generally smaller than the amplitude of the AW temperature seasonal cycle.

As opposed to temperature, the volume transport in the WSC (Figure 6b) shows strong variability on a monthly scale, with a maximum transport of 12–15 Sv in individual months (usually in winter). Variability in the WSC volume transport is nearly exclusively determined by transport variations in the offshore branch. Month-to-month variations in the volume transport in the WSC core are of the order of 1 Sv (compared with the long-term mean of 1.8 Sv), and annual means are nearly constant (~2 Sv), with slightly lower values in the years 2006–2008. Annual means of volume transport in the offshore branch can differ by up to 3–4 Sv. These differences may result from the interannual variability in large-scale atmospheric forcing (particularly in winter), as well as from short-term spatial shifts of the western WSC boundary and a varying intensity of the westward recirculation.

The first warming period in Fram Strait (Figure 6a) coincides with a large volume transport in the WSC (Figure 6b), in particular during winter 1999/2000, when inflow was strong between late summer and early spring. In contrast, the second, stronger warming event (Figure 6a) was not accompanied by a significant increase in volume transport (Figure 6b), except for 2007, when stronger than average inflow was observed in late winter (March–April). On the other hand, volume transport in summer 2006 did not demonstrate the typical summer minimum, because it remained close to the annual average. As a result, inflow of the AW in the WSC (Figure 6c) was relatively high in autumn and winter 2006/2007 (maximum in December and January) and dropped significantly in summer 2007, when record low volume transport was observed in the WSC.

Some authors have reported an extraordinarily strong AW inflow during the second warming period (e.g. Walczowski and Piechura, 2007). However, it can be attributed to the month-to-month variability in the volume transport because their study is based on hydrographic sections measured in July 2006. During that month, the volume transport in the WSC was indeed higher than average (the second highest in the measured time-series), but in the preceding and following summer and autumn months, it was close to average.

The early winter, maximum of AW inflow in 2006 was attributable to wider occupation of the section by the warm AW rather than increased volume transport. When the volume flux peaked in March–April 2007, the AW inflow was actually near its long-term average because of a seasonal minimum in the AW temperature.

## Long-term (decadal) trends

In the AW, a statistically significant (at a 99% significance level) positive trend of 0.06°C year$^{-1}$ was found in both WSC branches. This is equivalent to a temperature increase of 0.8°C over 13 years of observations. However, it is somewhat smaller than the AW temperature trend found for the period between the coldest observed values in 1997 and the temperature peak in 2006 (0.1°C year$^{-1}$, significant at the 99% level), which suggested an increase of 1°C over 10 years. This underlines the fact that trends based on relatively short time-series should be considered carefully because they may represent variability in a shorter 4- to 6-year band (as observed in Fram Strait) rather than a real long-term trend. No statistically significant trend was found in the WSC total and AW volume transport, agreeing with the findings of Skagseth *et al.* (2008) who found no trend in the AW volume transport in the upstream NwASC.

Our observational time-series are too short to address multidecadal variability. By comparing decade-to-decade variations, it may be concluded that in the past decade, there was an increase of AW temperature by ~0.5°C while volume transport in the WSC decreased slightly compared with the previous decade.

## Discussion and conclusions

The main feature observed in the northern Fram Strait from 1997 to 2010 was an increase in the temperature of the AW advected from the North Atlantic towards the Arctic Ocean. These warm anomalies originated from the upstream basins and travelled with a time-lag northwards, being modified along the way by ocean–atmosphere exchanges and lateral mixing with ambient waters. In the North Atlantic and southern Norwegian Sea, a remarkable increase in the AW temperature and salinity has been observed since the 1990s (Turrell *et al.*, 2003). At the Svinøy section in the Norwegian Sea, the first warm event can be recognized between 1997 and 1998 and was followed by the second temperature increase, which started around 2002/2003 (Orvik and Skagseth, 2005; Skagseth *et al.*, 2008). The first warm anomaly arrived at Fram Strait in 1998/1999, and the second one was observed there after 2004. This implies a time-lag of 1–2 years for the advection of anomalous waters from the North Atlantic to the northern Fram Strait, much slower than the mean speed of the slope current (the NwASC and farther north the WSC). The results of Holliday *et al.* (2008) show that a coherent anomalous temperature and salinity signal can be found all round the northeastern North Atlantic, from the Rockall Trough to the northern Fram Strait.

Anomalies in the core and offshore WSC branches have different signatures owing to their origin from two branches of the NwAC. Mauritzen *et al.* (2011) show that the volume transport in the eastern slope current (NwASC) has a main temperature mode in the range 8.5–9°C, whereas in the AW originating from the western baroclinic branch of the NwAC, the volume transport is in the main temperature mode of 7.5–8°C. Different advection time-scales for these two branches result in a different cooling rate of the AW before it encounters Polar Water in Fram Strait. There is

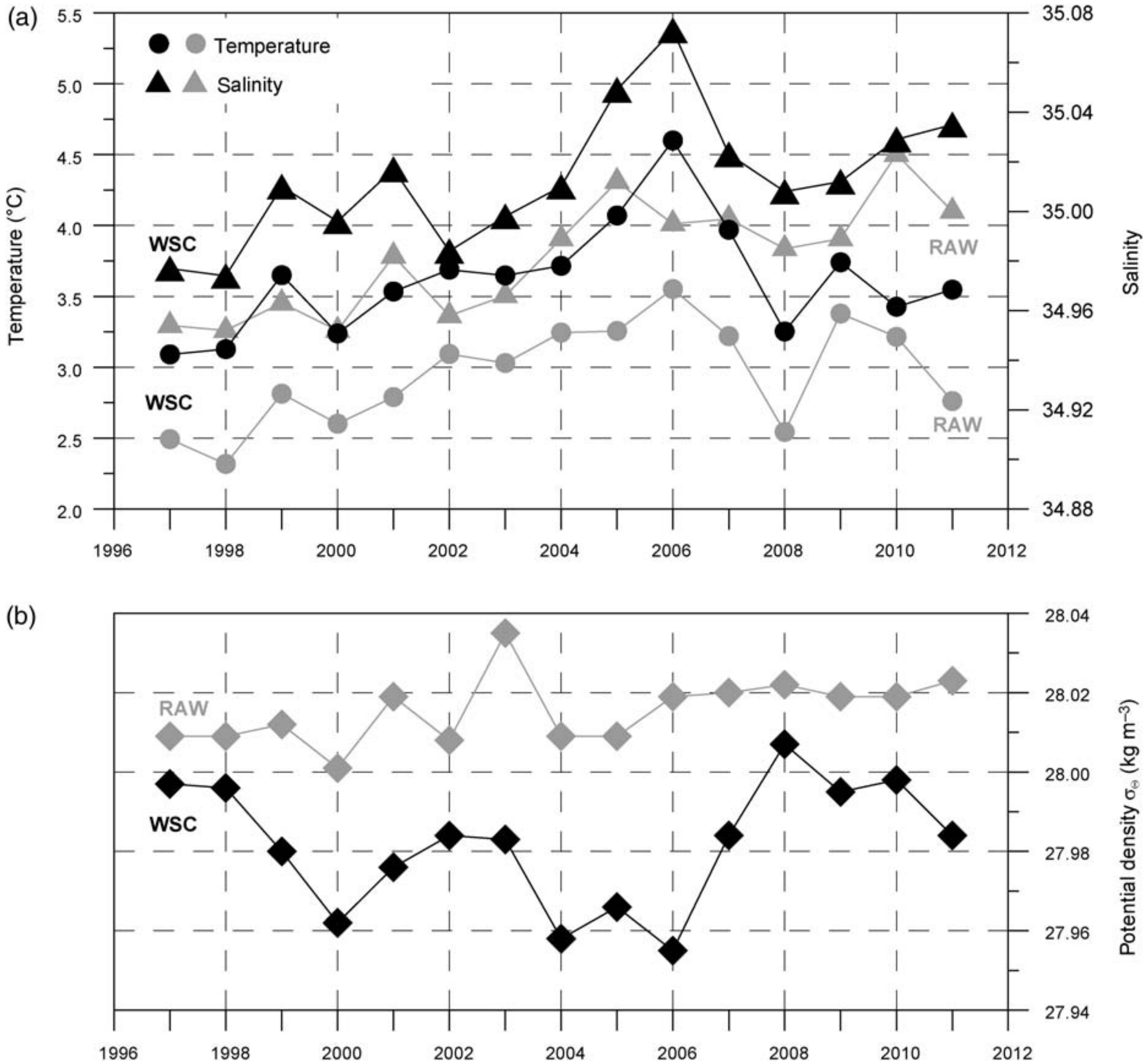


**Figure 7.** (a) Mean temperature (circles) and salinity (triangles), and (b) potential density of the AW layer in the WSC (black line) and RAW (grey line) measured during summer/autumn hydrographic surveys. In hydrographic fields from CTD measurements, the AW layer was defined as temperature $>2°C$ and salinity $>34.9$.

also a significant lateral eddy exchange between both branches (Rossby *et al.*, 2009; Andersson *et al.*, 2011), which implies that the two branches are not distinct in a Lagrangian sense. A similar situation is found between two branches of the WSC in Fram Strait. The strong lateral exchange is caused by vortices generated by barotropic instability in the WSC core (Teigen *et al.*, 2010) as well by baroclinic instability in the offshore branch (Teigen *et al.*, 2011). The lateral heat exchange through vortices in the WSC can at times be stronger than the heat exchange with the atmosphere.

The warm anomalies passing through Fram Strait can be traced farther in the Arctic Ocean along the boundary of the Eurasian Basin. Polyakov *et al.* (2005) found a temperature anomaly in the eastern Eurasian Basin in 2004. This anomaly originated in the North Atlantic and took ~1.5 years to propagate from the Norwegian Sea to the Fram Strait region (the first warm anomaly observed there between 1997 and 1999), and an additional ~4.5–5 years to reach the Laptev Sea slope. A recent study by Polyakov *et al.* (2010) shows that the warm pulse of AW that entered the Arctic Ocean in the early 1990s finally reached the Canada Basin during the 2000s. The second warm pulse that entered the Arctic Ocean in the mid-2000s has moved through the Eurasian Basin and is *en route* downstream. Those authors also claim a possibility of the uptake of anomalous AW heat by overlying layers, with possible implications for an already reduced Arctic ice cover. However, the possible impact of warmer Atlantic water on the shrinking sea-ice cover in the Arctic Ocean is a subject of controversy between different authors, because the Atlantic layer in the Arctic Ocean is shielded from the sea ice by the cold halocline, which suppresses upward heat flux.

Although the potential link between the anomalously warm AW inflow and sea-ice concentration in the Arctic Ocean is not clearly established, the strong influence of the AW temperature on sea-ice conditions around Svalbard is well documented. Cokelet *et al*. (2008) showed that the region north of Svalbard is characterized by large ocean–atmosphere heat flux, reaching a maximum of 520 W $m^{-2}$. This region, called Whaler's Bay, is where the main direct interactions between warm Atlantic water and sea ice take place (Rudels, 2010). Rudels (2010) showed that the warmer inflowing Atlantic water implies not only that more heat is released when cooled to freezing temperature, but also that more of the lost heat is going to ice-melt. The effect of a higher AW temperature in the WSC would then be to increase the ice-melt and the area of open water north of Svalbard more than can be anticipated from just the increase in AW temperature alone. Observational support based on summer hydrographic measurements west of Svalbard were also presented by Walczowski and Piechura (2011), who suggested a negative correlation between AW temperature and sea-ice concentration north of Svalbard.

Another potential impact of the anomalously warm events entering the Arctic Ocean arises from the fact that in terms of seawater density, positive temperature anomalies are not fully compensated for by changes in salinity, and as a consequence density anomalies can arise (Karcher *et al*., 2011). Although the quality of salinity data from the moored array is not sufficient to reveal these density variations, hydrographic measurements along the same section repeated annually in summer do allow an estimate of summer-to-summer variation in the AW mean salinity and density. Figure 7 shows the mean temperature, salinity, and density of the AW in the WSC and recirculation area (RAW). It is clear that, although the overall variations in salinity follow the temperature variability in the WSC and within the recirculating AW, the temperature peaks do not necessarily coincide with salinity maxima. As a result, density minima arise like that observed between 2004 and 2006 (Figure 7). Karcher *et al*. (2011) argue that such negative density anomalies have the potential to survive a circumnavigation of the Arctic Ocean and could influence the dense overflows into the North Atlantic.

The warm AW waters recirculating directly in Fram Strait or just north of the strait join the EGC and influence the properties of the intermediate waters carried south to the Nordic Seas and the North Atlantic. In recent decades, the cold dome structure in the Greenland Sea Gyre was replaced by a two-layer structure separated by a temperature maximum (Budéus and Ronski, 2009). The interface between the layers has descended with time, and the upper layer volume has increased, being fed by the Polar Water and AW derivatives. The upper layer of the Greenland Sea Gyre can potentially be influenced by the warmer AW recirculation in Fram Strait.

The AW in the WSC core water has the greatest chance to travel far into the Arctic Ocean, so the AW temperature and inflow variations in this branch may have the greatest impact on properties of the AW in the Arctic Ocean Boundary Current. On the other hand, variations in the offshore WSC branch have the greatest influence on the direct recirculation of the AW and also on the ocean–atmosphere heat fluxes in the region north of Fram Strait. Their potential impact is likely to be the strongest on the properties of the Arctic outflow towards the North Atlantic. Therefore, changes in AW properties and transport in both WSC branches in Fram Strait are not only of regional importance but may also potentially influence large-scale circulation in the North Atlantic and Arctic Ocean.

## Acknowledgements

The long-term maintenance of moorings in Fram Strait was supported by the EU project ASOF–N (Arctic–Subarctic Ocean Flux Array for European Climate–North; contract number EVK2-CT-200200139), the EU Integrated Project DAMOCLES (Developing Arctic Modelling and Observing Capabilities for Long-term Environment Studies, contract number 018509GOCE), and the EU Collaborative Project ACOBAR (Grant Agreement no. 212887). We thank all the research and sea-going staff who helped with the mooring operations during many years of fieldwork.

## References

Andersson, M., Orvik, K. A., LaCasce, J., Koszalka, I., and Mauritzen, C. 2011. Variability of the Norwegian Atlantic Current and associated eddy field from surface drifters. Journal of Geophysical Research, 116: C08032, doi:10.1029/2011JC007078.

Bersch, M., Yashayaev, I., and Koltermann, K. P. 2007. Recent changes of the thermohaline circulation in the subpolar North Atlantic. Ocean Dynamics, 57: 223–235.

Budéus, G., and Ronski, S. 2009. An integral view of the hydrographic development in the Greenland Sea over a decade. The Open Oceanography Journal, 3: 8–39.

Cokelet, E. D., Tervalon, N., and Bellingham, J. G. 2008. Hydrography of the West Spitsbergen Current, Svalbard branch: autumn 2001. Journal of Geophysical Research, 113: C01006, doi:10.1029/2007JC004150.

Dmitrenko, I. A., Polyakov, I. V., Kirillov, S. A., Timokhov, L. A., Frolov, I. E., Sokolov, V. T., Simmons, H. L., *et al*. 2008. Toward a warmer Arctic Ocean: spreading of the early 21st century Atlantic Water warm anomaly along the Eurasian Basin margins. Journal of Geophysical Research, 113, C05023, doi:10.1029/2007JC004158.

Fahrbach, E., Meincke, J., Østerhus, S., Rohardt, G., Schauer, U., Tverberg, V., and Verduin, J. 2001. Direct measurements of volume transports through Fram Strait. Polar Research, 20: 217–224.

Fahrbach, E., Rohardt, G., and Sieger, R. 2007. 25 years of Polarstern hydrography (1982–2007). 5. Alfred Wegener Institute for Polar and Marine Research, Bremerhaven. doi:10013/epic.30213. d001.

Furevik, T. 2001. Annual and interannual variability of Atlantic Water temperatures in the Norwegian and Barents Seas: 1980–1996. Deep Sea Research I, 48: 383–404.

Hátún, H., Sandø, A. B., and Drange, H. 2005. Influence of the Atlantic Subpolar Gyre on the thermohaline circulation. Science, 309: 1841–1844.

Holliday, N. P., Hughes, S. L., Bacon, S., Beszczynska-Möller, A., Hansen, B., Lavin, A., Loeng, H., *et al*. 2008. Reversal of the 1960s to 1990s freshening trend in the northeast North Atlantic and Nordic Seas. Geophysical Research Letters, 35: L03614, doi:10.1029/2007GL032675.

Holliday, N. P., Hughes, S. L., and Beszczynska-Möller, A. (eds). 2009. ICES Report on Ocean Climate 2008. ICES Cooperative Research Report, 298. 66 pp.

Karcher, M., Beszczynska-Möller, A., Kauker, F., Gerdes, R., Heyen, S., Rudels, B., and Schauer, U. 2011. Arctic Ocean warming and its consequences for the Denmark Strait overflow. Journal of Geophysical Research, 116: C02037, doi:10.1029/2010JC006265.

Karcher, M. J., Gerdes, R., Kauker, F., and Köberle, C. 2003. Arctic warming: evolution and spreading of the 1990s warm event in the Nordic seas and the Arctic Ocean. Journal of Geophysical Research, 108(C2): 3034, doi:10.1029/2001JC001265.

Manley, T. O. 1995. Branching of Atlantic Water within the Greenland–Spitsbergen Passage: an estimate of recirculation. Journal of Geophysical Research, 100(C10): 20627–20634.

Mauritzen, C., Hansen, E., Andersson, E. M., Berx, B., Beszczynska-Möller, A., Burud, I., Christensen, K. H., *et al.* 2011. Closing the loop—approaches to monitoring the state of the Arctic Mediterranean during the International Polar Year 2007–2008. Progress in Oceanography, 90: 1–4.

Mork, K. A., and Skagseth, Ø. 2010. A quantitative description of the Norwegian Atlantic Current by combining altimetry and hydrography. Ocean Science, 6: 901–911.

Nøst, O. A., and Isachsen, P. E. 2003. The large-scale time-mean ocean circulation in the Nordic Seas and Arctic Ocean estimated from simplified dynamics. Journal of Marine Research, 61: 175–210.

Orvik, K. A., and Niiler, P. 2002. Major pathways of Atlantic water in the northern North Atlantic and Nordic Seas toward Arctic. Geophysical Research Letters, 29: 1896, doi:10.1029/2002GL015002.

Orvik, K. A., and Skagseth, Ø. 2005. Heat flux variations in the eastern Norwegian Atlantic Current toward the Arctic from moored instruments, 1995–2005. Geophysical Research Letters, 32: L14610, doi:10.1029/2005GL023487.

Padman, L., Plueddemann, A. J., Muench, R. D., and Pinkel, R. 1992. Diurnal tides near the Yermak Plateau. Journal of Geophysical Research, 97(C8): 12639–12652.

Polyakov, I. V., Beszczynska, A., Carmack, E. C., Dmitrenko, I. A., Fahrbach, E., Frolov, I. E., Gerdes, R., *et al.* 2005. One more step toward a warmer Arctic. Geophysical Research Letters, 32: L17605, doi:10.1029/2005GL023740.

Polyakov, I. V., Timokhov, L. A., Alexeev, V. A., Bacon, S., Dmitrenko, I. A., Fortier, L., Frolov, I. E., *et al.* 2010. Arctic Ocean warming contributes to reduced polar ice cap. Journal of Physical Oceanography, 40: 2743–2756.

Rossby, T., Ozhigin, V., Ivshin, V., and Bacon, S. 2009. An isopycnal view of the Nordic Seas hydrography with focus on properties of the Lofoten Basin. Deep Sea Research I, 56: 1955–1971.

Rudels, B. 2010. Constraints on exchanges in the Arctic Mediterranean—do they exist and can they be of use. Tellus, 62A: 109–122.

Rudels, B., Björk, G., Nilsson, J., Winsor, P., Lake, I., and Nohr, C. 2005. The interactions between waters from the Arctic Ocean and the Nordic Seas north of Fram Strait and along the East Greenland Current: results from the Arctic Ocean–02 Oden expedition. Journal of Marine Systems, 55: 1–30.

Saloranta, T. M., and Haugan, P. M. 2004. Northward cooling and freshening of the warm core of the West Spitsbergen Current. Polar Research, 23: 79–88.

Schauer, U., Beszczynska-Möller, A., Walczowski, W., Fahrbach, E., Piechura, J., and Hansen, E. 2008. Variation of measured heat flow through the Fram Strait between 1997 and 2006. *In* Arctic–Subarctic Ocean Fluxes: Defining the Role of the Northern Seas in Climate, pp. 65–85. Ed. by R. R. Dickson, J. Meincke, and P. Rhines. Springer, Dordrecht.

Schauer, U., Fahrbach, E., Osterhus, S., and Rohardt, G. 2004. Arctic warming through the Fram Strait: oceanic heat transport from 3 years of measurements. Journal of Geophysical Research, 109(C06026), doi:10.1029/2003JC001823.

Schauer, U., Loeng, H., Rudels, B., Ozhigin, V. K., and Dieck, W. 2002. Atlantic Water flow through the Barents and Kara Seas. Deep Sea Research I, 49: 2281–2298.

Schlichtholz, P., and Houssais, M-N. 2002. An overview of the Θ–S correlation in Fram Strait based on the MIZEX 84 data. Oceanologia, 44: 243–272.

Skagseth, Ø., Furevik, T., Ingvaldsen, R., Loeng, H., Mork, K. A., Orvik, K. A., and Ozhigin, V. 2008. Volume and heat transports to the Arctic Ocean via the Norwegian and Barents seas. *In* Arctic–Subarctic Ocean Fluxes: Defining the Role of the Northern Seas in Climate, pp. 45–64. Ed. by R. R. Dickson, J. Meincke, and P. Rhines. Springer, Dordrecht.

Skagseth, Ø., Orvik, K. A., and Furevik, T. 2004. Coherent variability of the Norwegian Atlantic Slope Current derived from TOPEX/ERS altimeter data. Geophysical Research Letters, 31: L14304, doi:10.1029/2004GL020057.

Smedsrud, L. H., Ingvaldsen, R., Nilsen, J. E. Ø., and Skagseth, Ø. 2010. Heat in the Barents Sea: transport, storage, and surface fluxes. Ocean Science, 6: 219–234.

Teigen, S. H., Nilsen, F., and Gjevik, B. 2010. Barotropic instability in the West Spitsbergen Current. Journal of Geophysical Research, 115: C07016, doi:10.1029/2009JC005996.

Teigen, S. H., Nilsen, F., Skogseth, R., Gjevik, B., and Beszczynska-Moeller, A. 2011. Baroclinic instability in the West Spitsbergen Current. Journal of Geophysical Research, 116(C07012), doi:10.1029/2011JC006974.

Turrell, W. R., Hansen, B., Hughes, S., and Østerhus, S. 2003. Hydrographic variability during the decade of the 1990s in the Northeast Atlantic and southern Norwegian Sea. ICES Marine Science Symposia, 219: 111–120.

Tverberg, V., and Nøst, O. A. 2009. Eddy overturning across a shelf edge front: Kongsfjorden, west Spitsbergen. Journal of Geophysical Research, 114: C04024, doi:10.1029/2008JC005106.

von Schuckmann, K., Gaillard, F., and Le Traon, P. Y. 2009. Global hydrographic variability patterns during 2003–2008. Journal of Geophysical Research, 114, C09007, doi:10.1029/2008jc005237.

Walczowski, W., and Piechura, J. 2007. Pathways of the Greenland Sea warming. Geophysical Research Letters, 34: L10608, doi:10.1029/2007GL029974.

Walczowski, W., and Piechura, J. 2011. Influence of the West Spitsbergen Current on the local climate. International Journal of Climatology, 31: 1088–1093.

Walczowski, W., Piechura, J., Osinski, R., and Wieczorek, P. 2005. The West Spitsbergen Current volume and heat transport from synoptic observations in summer. Deep Sea Research I, 52: 1374–1991.


*Handling editor: Bill Turrell*